

## CONSTRAINING THE TRANSPORT PROCESSES IN STELLAR INTERIORS WITH RED GIANT STARS

Lagarde N.<sup>1</sup>, Eggenberger P.<sup>2</sup>, Miglio, A.<sup>1,3</sup> and Montalbàn, J.<sup>4</sup>

**Abstract.** Recent asteroseismic observations have led to the determination of the core rotation rate for a large number of red-giant stars by the study of rotational frequency splittings of  $l=1$  mixed modes. We present how these observed core rotation rates can constrain the efficiency of an additional unknown physical transport process occurring in red-giant stars. We compare theoretical models including rotation-induced mixing and an additional viscosity in the transport of angular momentum, with asteroseismic observations during the red giant branch and the clump.

Keywords: Asteroseismology, stars: structure, stars: evolution, stars: rotation, stars: interiors

### 1 Introduction

Red-giant stars are interesting targets to test and improve stellar evolution models. Numerous spectroscopic observations showed abundance anomalies in red giants brighter than the bump luminosity (e.g. Gratton et al. 2000; Smiljanic et al. 2009), which are not predicted by standard stellar models. Different transport processes have been proposed to understand the surface chemical properties of these stars. In particular, rotation-induced mixing, which changes the structure and chemical profiles during the main sequence but is not efficient enough to reproduce spectroscopic observations during the red giant branch (hereafter RGB Palacios et al. 2003, 2006). As shown by Charbonnel & Zahn (2007), thermohaline instability is a good candidate to explain abundance anomalies in low-mass red-giant stars. Charbonnel & Lagarde (2010) concluded that it is the dominating chemical transport process in low-mass red-giant stars ( $M < 2.0 M_{\odot}$ ), which governs their photospheric composition, while rotation-induced mixing with different initial velocities, explain surface abundances in more massive stars ( $M > 2.0 M_{\odot}$ ).

In recent years, a large number of asteroseismic data have been obtained for different kinds of stars, which allowed the detection and characterization of solar-like oscillations in a large number of red giants by space missions (e.g. De Ridder et al. 2009). Thousands of evolved stars (subgiant, giant and clump stars) have been already observed by CoRoT (Baglin et al. 2006) and *Kepler* (Borucki et al. 2010), allowing access to the properties of the stellar interiors of red giant stars.

### 2 Asteroseismology: new tool to improve stellar models

Determination of individual frequencies represents an excellent opportunity to deduce from asteroseismology stellar mass and radius (Beck et al. 2012), as well as distance and age (see Chaplin & Miglio 2013, and references therein). In addition, asteroseismology brings key information on the stellar structure with different acoustic radius (total, at the base of convective envelope or the base of the helium second ionization region), and with the period spacing of gravity modes for  $l=1$ . As proposed by Bedding et al. (2011) and Mosser et al. (2011),

---

<sup>1</sup> School of Physics and Astronomy, University of Birmingham, Edgbaston, Birmingham B15 2TT, UK

<sup>2</sup> Geneva Observatory, University of Geneva, Chemin des Maillettes 51, 1290 Versoix, Switzerland

<sup>3</sup> Stellar Astrophysics Centre (SAC), Department of Physics and Astronomy, Aarhus University, Ny Munkegade 120, 8000 Aarhus C, Denmark

<sup>4</sup> Institut d'Astrophysique et de Géophysique, Université de Liège, Allée du 6 Août, Bât. B5c, 4000 Liège, Belgium

this quantity provides the evolutionary state of giant stars, distinguishing RGB and clump stars.

Moreover, thanks to asteroseismology, we can now determine the internal rotation of giant stars (Deheuvels et al. 2012, 2014; Beck et al. 2012; Mosser et al. 2012), and then test models of transport of angular momentum (Eggenberger et al. 2012; Ceillier et al. 2013; Marques et al. 2013). As underlined by Eggenberger et al. (2012) in the case of giant star KIC8366239, a discrepancy exists between the rotation profile deduced from asteroseismic observations and the profiles predicted from models including shellular rotation and related meridional flows and turbulence. They show that a most powerful mechanism is in action to extract angular momentum from the core of this star, and other red giant stars.

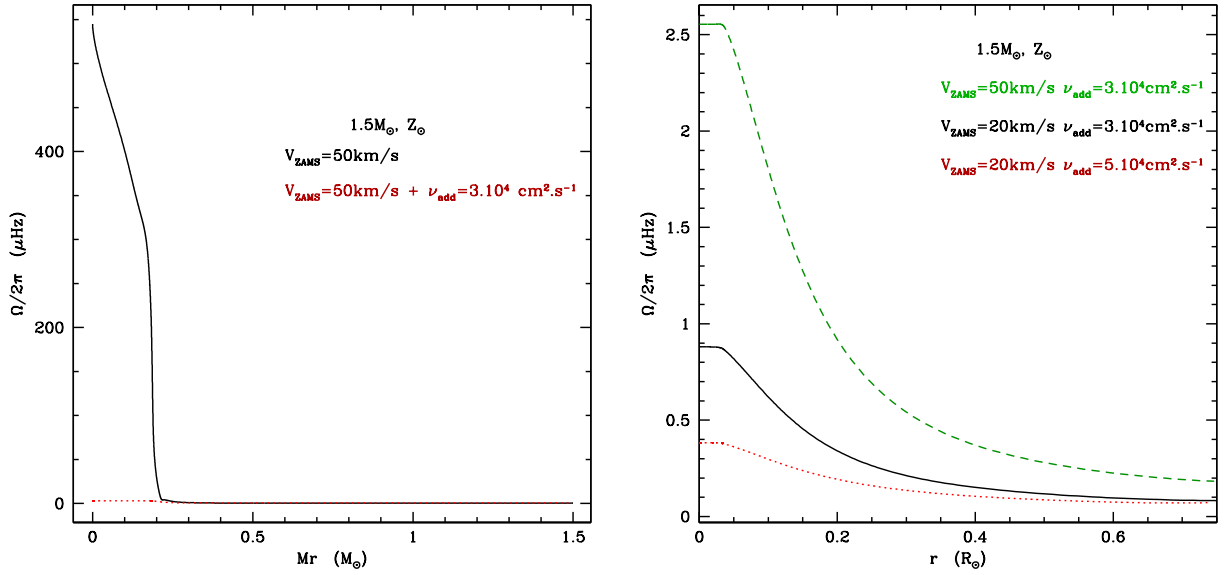


**Fig. 1.** Theoretical rotation profile in  $1.5M_{\odot}$  at solar metallicity at the beginning of the red giant branch ( $R_{\star}=4R_{\odot}$ ): **Left:** in the case of standard rotating model with  $V_{ZAMS}=50\text{km}\cdot\text{s}^{-1}$  (black line) and including impact of an additional viscosity ( $V_{ZAMS}=50\text{km}\cdot\text{s}^{-1}$ ,  $\nu_{add}=3.10^4\text{ cm}^2\cdot\text{s}^{-1}$ , red dashed line); **Right panel** including an additional viscosity and two initial velocity at the ZAMS ( $V_{ZAMS}=50\text{km}\cdot\text{s}^{-1}$ ,  $\nu_{add}=3.10^4\text{ cm}^2\cdot\text{s}^{-1}$ , green dashed line); ( $V_{ZAMS}=20\text{km}\cdot\text{s}^{-1}$ ,  $\nu_{add}=3.10^4\text{ cm}^2\cdot\text{s}^{-1}$ , black solid line), and ( $V_{ZAMS}=20\text{km}\cdot\text{s}^{-1}$ ,  $\nu_{add}=5.10^4\text{ cm}^2\cdot\text{s}^{-1}$ , red dashed line)

As proposed by Eggenberger et al. (2012) to quantify the efficiency of this additional mechanism in the RGB stars, we include an additional viscosity in the equation of the transport of angular momentum, corresponding to an additional physical process for the transport of angular momentum in radiative zones (Eq 2.1):

$$\underbrace{\rho \frac{d(r^2\Omega)}{dt}}_{\text{stellar contraction/expansion}} = \underbrace{\frac{1}{5r^2} \frac{\partial}{\partial r} (\rho r^4 \Omega U_r)}_{\text{advection of angular momentum by meridional circulation}} + \underbrace{\frac{1}{r^2} \frac{\partial}{\partial r} \left( r^4 \rho (D + \nu_{add}) \frac{\partial \Omega}{\partial r} \right)}_{\text{diffusion effect of shear-induced turbulence and additional viscosity}}, \quad (2.1)$$

with  $r$  the stellar radius,  $\rho$  the density,  $\nu_{add}$  the additional viscosity,  $\Omega$  the angular velocity, and  $U_r$  the vertical component of meridional circulation velocity.

This corresponds well to the two main mechanisms currently proposed to efficiently extract angular momentum from the central core of a solar-type star having a strong impact on the transport of angular momentum. We use the stellar evolutionary code *STAREVOL* (e.g. Palacios et al. 2006; Lagarde et al. 2012) to compute models presented here, including rotation-induced mixing all along the evolution.

Figure 1 displays effects of additional viscosity and different initial velocity on the theoretical rotation profiles for  $1.5M_{\odot}$  model at solar metallicity for a given stellar radius on the red giant branch. We underline on

the left panel of Fig.1 the strong impact of  $\nu_{add}$  on the core rotation rate which decreases by three orders of magnitude when we consider  $\nu_{add}$  in the transport of angular momentum. In addition, at a given velocity an increase in  $\nu_{add}$  results in a more efficient transport of angular momentum, hence in a flatter rotation profile in the radiative zone (right panel of Fig.1).  $\nu_{add}$  allows us to determine the efficiency of an additional physical process needed on the RGB, which can be constrained thanks to asteroseismic measurements.

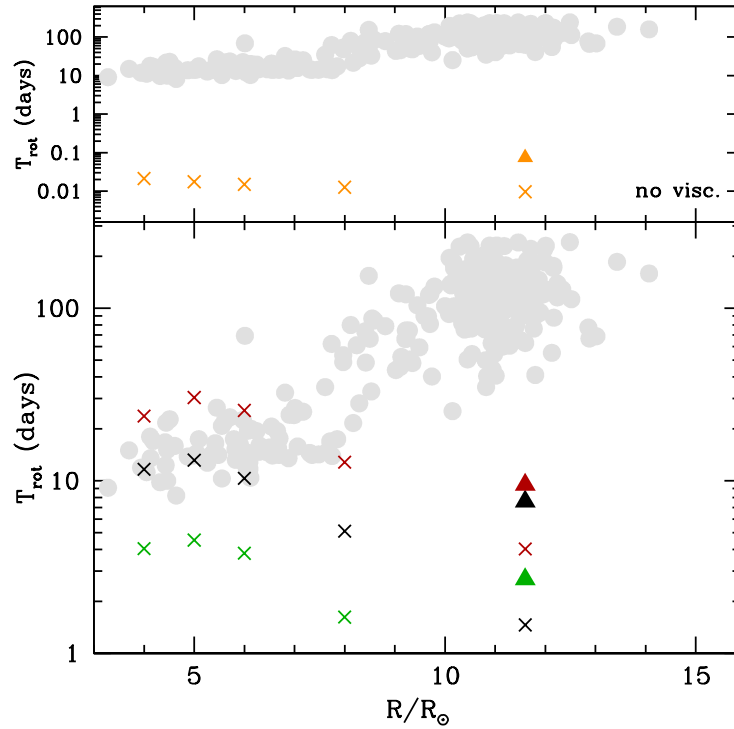


**Fig. 2.** Theoretical rotation periods of the core as a function of stellar radius of  $1.5M_{\odot}$  along the RGB (cross) and during the clump (triangle), compared to observations in field stars observed by Kepler from Mosser et al. (2012, , grey dots). Models follow standard rotating model (no viscosity, orange symbols), and including an additional viscosity at two initial velocities ( $V_{ZAMS}=50\text{km.s}^{-1}$ ,  $\nu_{add}=3.10^4 \text{ cm}^2.\text{s}^{-1}$ , red symbols) ; ( $V_{ZAMS}=20\text{km.s}^{-1}$ ,  $\nu_{add}=3.10^4 \text{ cm}^2.\text{s}^{-1}$ , black symbols), and ( $V_{ZAMS}=20\text{km.s}^{-1}$ ,  $\nu_{add}=5.10^4 \text{ cm}^2.\text{s}^{-1}$ , green symbols)

Figure 2 shows theoretical rotation period of the core for  $1.5 M_{\odot}$  along the RGB and during the clump, compared to observations in field stars observed by *Kepler* from Mosser et al. (2012). In the upper panel, orange symbols represent models with rotation ( $V_{ZAMS} = 50 \text{ km.s}^{-1}$ ), and without  $\nu_{add}$ , and clearly shows that classical rotating models cannot represent observed core rotation rate in red giant stars, with predicted periods 2 to 3 orders of magnitude lower than observed. On the other hand, models at constant  $\nu_{add}$  reproduce very well observations at the beginning of the RGB (Fig.2, lower panel). Observations show an increase of the core rotational period of giants as stars evolve, contrary to theoretical models (see also Fig. 2 and Cantiello et al. 2014). This implies an increase of the efficiency to transport the angular momentum along the red giant branch. However, we remark the same disagreement for clump stars (triangles on Fig.2), the observed and theoretical ratios between core rotational period of clump and RGB stars are slightly the same.

### 3 Conclusions

Thanks to asteroseismology, we can quantify the efficiency of an additional transport mechanism for the angular momentum along the red giant branch and during the He-burning. Observations by *Kepler* show an increase of this efficiency all along the red giant branch which is not reproduced by stellar models. Models used in this study including rotation-induced mixing all along the evolution of low-mass stars, will be useful to interpret

observations from *Kepler* in field stars, and particularly in open clusters. A detailed study of theoretical models and individual frequencies for giant stars will be discussed in a forthcoming paper (Lagarde et al 2014 in prep.)

NL acknowledges financial support from Marie Curie Intra-european fellowship (FP7-PEOPLE-2012-IEF)

## References

- Baglin, A., Auvergne, M., Boisnard, L., et al. 2006, in 36th COSPAR Scientific Assembly, Vol. 36, 3749
- Beck, P. G., Montalbán, J., Kallinger, T., et al. 2012, *Nature*, 481, 55
- Bedding, T. R., Mosser, B., Huber, D., et al. 2011, *Nature*, 471, 608
- Borucki, W. J., Koch, D., Basri, G., et al. 2010, *Science*, 327, 977
- Cantiello, M., Mankovich, C., Bildsten, L., Christensen-Dalsgaard, J., & Paxton, B. 2014, *ApJ*, 788, 93
- Ceillier, T., Eggenberger, P., García, R. A., & Mathis, S. 2013, *A&A*, 555, A54
- Chaplin, W. J. & Miglio, A. 2013, *ARA&A*, 51, 353
- Charbonnel, C. & Lagarde, N. 2010, *A&A*, 522, A10+
- Charbonnel, C. & Zahn, J. 2007, *A&A*, 476, L29
- De Ridder, J., Barban, C., Baudin, F., et al. 2009, *Nature*, 459, 398
- Deheuvels, S., Doğan, G., Goupil, M. J., et al. 2014, *A&A*, 564, A27
- Deheuvels, S., García, R. A., Chaplin, W. J., et al. 2012, *ApJ*, 756, 19
- Eggenberger, P., Montalbán, J., & Miglio, A. 2012, *A&A*, 544, L4
- Gratton, R. G., Sneden, C., Carretta, E., & Bragaglia, A. 2000, *A&A*, 354, 169
- Lagarde, N., Romano, D., Charbonnel, C., et al. 2012, *A&A*, 542, A62
- Marques, J. P., Goupil, M. J., Lebreton, Y., et al. 2013, *A&A*, 549, A74
- Mosser, B., Barban, C., Montalbán, J., et al. 2011, *A&A*, 532, A86
- Mosser, B., Goupil, M. J., Belkacem, K., et al. 2012, *A&A*, 548, A10
- Palacios, A., Charbonnel, C., Talon, S., & Siess, L. 2006, *A&A*, 453, 261
- Palacios, A., Talon, S., Charbonnel, C., & Forestini, M. 2003, *A&A*, 399, 603
- Smiljanic, R., Gauderon, R., North, P., et al. 2009, *A&A*, 502, 267